ADVANCED ENERGY MATERIALS
www.advenergymat.de

A Hybridized Power Panel to Simultaneously Generate Electricity from Sunlight, Raindrops, and Wind around the Clock

*Li Zheng, Gang Cheng, Jun Chen, Long Lin, Jie Wang, Yongsheng Liu, Hexing Li, and Zhong Lin Wang**

With the solar panels quickly spreading across the rooftops worldwide, solar power is now very popular. However, the output of the solar cell panels is highly dependent on weather conditions, making it rather unstable. Here, a hybridized power panel that can simultaneously generate power from sunlight, raindrop, and wind is proposed and demonstrated, when any or all of them are available in ambient environment. Without compromising the output performance and conversion efficiency of the solar cell itself, the presented hybrid cell can deliver an average output of 86 mW m^{-2} from the water drops at a dripping rate of 13.6 mL s^{-1}, and an average output of 8 mW m^{-2} from wind at a speed of 2.7 m s^{-1}, which is an innovative energy compensation to the common solar cells, especially in rainy seasons or at night. Given the compelling features, such as cost-effectiveness and a greatly expanded working time, the reported hybrid cell renders an innovative way to realize multiple kinds of energy harvesting and as an useful compensation to the currently widely used solar cells. The demonstrated concept here will possibly be adopted in a variety of circumstances and change the traditional way of solar energy harvesting.

1. Introduction

The ongoing worldwide energy crisis and severe environmental problems caused by the rampant consumption of fossil fuels have become serious issues over the past decades.[1] Under these concerns, harvesting energy from the natural environment such as sunlight,[2,3] wind,[4] and mechanical vibration[5–7] has attracted great attentions as part of efforts to realize sustainable development of the human civilization. Over the past decades, a growing research effort has been devoted to developing the renewable and green energy technologies.[8,9] Among them, solar energy harvesting is one of the well-developed and fruitful technologies due to the low cost and superior performance.[10] The only element lacking is that the solar cell can only work well under the full sun. On cloudy, rainy days, or at night, the output of solar cell panels is always largely suppressed or even vanished.[11]

Since the recently developed triboelectric nanogenerator (TENG) has been widely studied to harvest various mechanical energies from the environment into electricity,[12–21] especially the water-related TENG has been experimentally demonstrated,[22,23] with the regards of solar cells being dysfunctional in bad weather conditions, here we reported a multifunctional solar cell panel by hybridization with a transparent dual-mode TENG. Consequently, it can not only harvest energy from sunlight, but also from light wind and natural raindrops. Given no compromise of the solar energy harvesting, the presented hybrid cell holds a greatly expanded working time and provides good output compensation except for solar energy. In a windy day, the hybrid cell, harvesting energy from ambient wind, can deliver an average output of 8 mW m^{-2} at a wind speed of 2.7 m s^{-1}. On a rainy day, harvesting energy from the dripping waterdrops, the hybrid cell can achieve an average output of 86 mW m^{-2} at a dripping rate of 13.6 mL s^{-1}. These functions render that the hybrid cell plays an important and compensative role in the current field of solar energy harvesting. Given a collection of advantages, such as being cost-effective, easy fabrication, greatly expanded working time without compromising the original solar energy harvesting, the presented hybrid cell is a unique and practical step toward a high efficiency ambient green energy harvesting with a lower production cost per watt.

Dr. L. Zheng, Dr. Y. S. Liu, Prof. H. X. Li
School of Mathematics and Physics
Shanghai University of Electric Power
Shanghai 200090, China
Dr. L. Zheng, Dr. G. Cheng, J. Chen, Dr. L. Lin, Dr. J. Wang, Prof. Z. L. Wang
School of Material Science and Engineering
Georgia Institute of Technology
Atlanta, GA 30332-0245, USA
E-mail: zlwang@gatech.edu
Dr. G. Cheng
Key Lab of Special Functional Materials
Henan University
Kaifeng 475004, China
Prof. Z. L. Wang
Beijing Institute of Nanoenergy and Nanosystems
Chinese Academy of Sciences
Beijing 100083, China

DOI: 10.1002/aenm.201501152

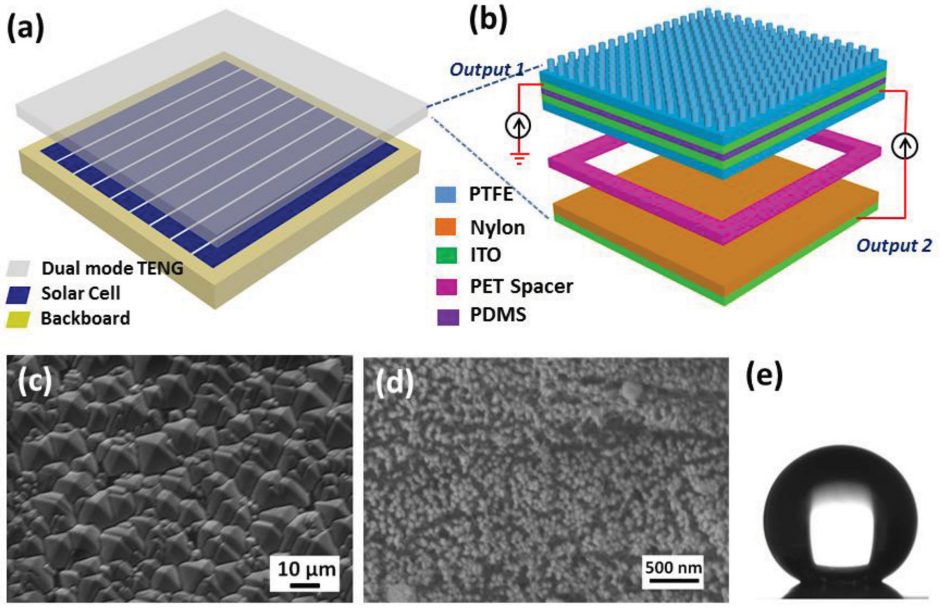

Figure 1. a) Schematic diagram of the as-fabricated hybridized power panel. b) An enlarged view to illustrate the dual-mode TENG in detail. A PET spacer was used to maintain the gap distance between the nether PTFE film and nylon film, integrating all the parts into a dual-mode TENG. The electricity generated from water TENG and contact TENG can be collected through the output 1 and output 2 of the dual-mode TENG. c) SEM image of the fabricated silicon-based solar cell surface with micro/nanostructured pyramids taken from a tilted view of 20°. d) SEM image of the PTFE thin film with hierarchical micro/nanostructures. e) The apparent contact angle of the PTFE thin film, indicating the film is superhydrophobic.

2. Results and Discussion

The reported hybridized power panel is mainly consisted of three parts: an acrylic backboard, a silicon-based solar cell, and a dual-mode TENG, as schematically depicted in **Figure 1**a. As the bottom part, acrylic is selected to be the backbone of the whole device owing to its decent strength, light weight, good machinability, and low cost. The middle part is a silicon-based solar cell ordinally consists of an Al film electrode, a p^+ back field layer, a p-type Si bulk layer, an n^+ emitter layer, SiN film, Ag grids, and an indium tin oxide (ITO) film electrode.[10] Micropyramidal morphology was created on the surface of the Si-based solar cell to enhance light absorption and suppress light reflectance so as to improve the light-electricity conversion efficiency of the solar cell. The top part is a dual-mode TENG which is an integration of a water TENG and a contact TENG using a spacer of PET, and the specific corresponding structure and electric output of this dual-mode TENG is schematically shown in Figure 1b. The detailed fabrication process of the Si solar cell and the hybridized power panel is described in the Experimental Section. A scanning electron microscopy (SEM) image of the Si solar cell surface is exhibited in Figure 1c, indicating that the surface is micropyramidal with a size range of 1–10 μm. The superhydrophobic polytetrafluoroethylene (PTFE) thin film was fabricated by using a homemade porous anodic Al oxide (AAO) template. Figure 1d shows an SEM image of the prepared PTFE film, where the surface of the PTFE film is composed of high-density nanorods, which will contain trapped air to reduce the actual contact area between the surface and water, contributing to the superhydrophobicity.[24] An apparent contact angle of 155° of the fabricated PTFE film is shown in Figure 1e, confirming that the surface is superhydrophobic (>150°).[25]

To examine the feasibility of the dual-mode TENG as a protection layer on solar cell surface, we first test the spectra transmittance of the dual-mode TENG. Figure S1a (Supporting Information) shows the spectra transmittance comparison of the dual-mode TENG with a 3 mm thick conventional glass, indicating that the fabricated dual-mode TENG is slightly more transparent than the conventional glass that is commercially used in industry in the visible light region. The *J*–*V* curves of fabricated Si solar cell integrated with the dual-mode TENG and conventional glass are also measured, respectively, as displayed in Figure S1b (Supporting Information). Under a solar light irradiation (100 mW cm^{-2}), the short-circuit current density (J_{sc}) of the hybrid cell is slightly higher than that of the traditional solar cell panel, revealing that the dual-mode TENG will not affect the function of the solar cell compared with the traditional ones. Moreover, the superhydrophobicity of PTFE thin film in water TENG can also render a self-cleaning property of the solar cell surface, which could keep the surface from dust in the air and always provide a transparent protection layer, maintaining the standard working efficiency of the hybridized power panel.

The fundamental working principle of dual-mode TENG is based on a sequential process of contact electrification and electrostatic induction,[26] which can be depicted separately as a water TENG (**Figure 2**a) and a contact TENG (Figure 2b). To apply this technique in real life and achieve high energy conversion efficiency, the water TENG and contact TENG are operated in single-electrode and dual-electrode mode, respectively. Previous studies have pointed out that contact electrification of water with pipe/air can cause triboelectric charges in water,[27,28] and the polarity of the triboelectric charge in water depends on the material that the water contact with.[22] For simplification, several randomly falling water drops carrying positive charges are chosen

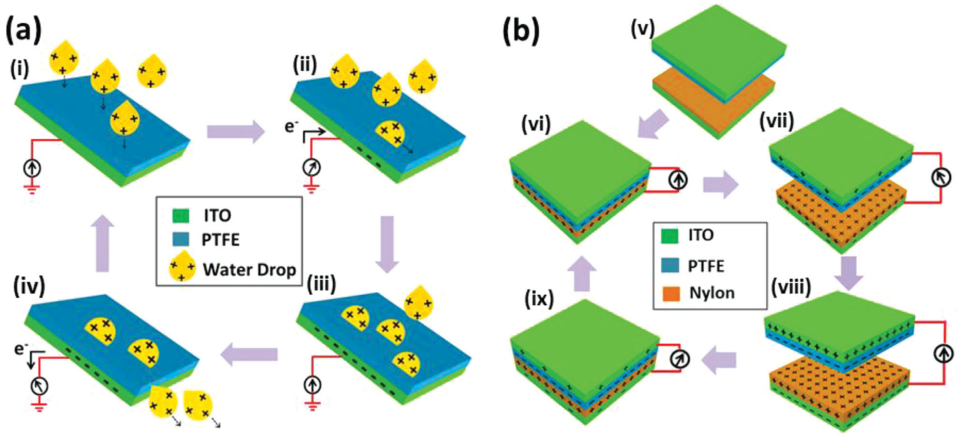

Figure 2. Schematic diagram of the working mechanism of the a) water TENG and b) contact TENG for rain and wind energy harvesting. (ii) When several positively charged water drops contact the hydrophobic PTFE surface, (iii) a positive electric potential difference will be formed and causes the electron to flow from the ground to the ITO electrode, finally reaching equilibrium. (iv) Once the charged water drops leave the PTFE surface, a negative electric potential difference will be formed and forces the electrons to flow from the ITO electrode to the ground, until reaching another equilibrium. (vi) On the other hand, the impact force from the water drops also makes the nether PTFE film contact with nylon film, causing the PTFE and nylon film charged surfaces. (vii) As the water drops leave, the contacted surfaces are separated due to their own elastic resilience, then a negative electric potential difference between the upper and nether ITO electrodes will be established. (viii) This causes the electrons to flow from the nether ITO electrode to upper ITO electrode, finally reaching equilibrium. (ix) When water drops fall again and make the PTFE film contact the nylon film, a positive EPD will be established and forces the electrons to flow from the upper ITO electrode to the ITO electrode, (vi) until reaching another equilibrium. As for wind contact TENG working mechanism, it is exactly the same with water contact TENG except for the driving force.

here to illustrate the dynamic process of energy transformation. When these randomly positively charged water drops reach the PTFE surface (ii), a positive electric potential difference (EPD) will be established between the ITO electrode of PTFE film and the ground. This causes the electrons to flow from the ground to the ITO electrode till the EPD is balanced (iii). Once the charged water drops leave the PTFE film surface, a negative EPD will be formed, forcing the electrons to flow from the ITO electrode to the ground (iv), until achieving equilibrium. When charged water drops contact and leave the PTFE film periodically, continuous electric output can be generated from output 1 of this dual-mode TENG. It is worth noting that the magnitude of electric output from output 1 is determined by the charge density on water drop surface, while charge density on water drop surface is affected by different weather conditions.

Meanwhile, the impact force from a water drop as it falls down onto the dual-mode TENG also drives the contact TENG to generate electricity. The impact force will bring the PTFE film into contact with the nylon film, and then surface charge transfer takes place at the contact area due to triboelectric effect. According to the triboelectric series, electrons are injected from nylon to PTFE film, resulting in net negative charges at PTFE surface and net positive charges at nylon surface.[29–31] Since they are only confined at the surfaces, charges with opposite signs coincide at almost the same plane, generating no EPD between the two corresponding ITO electrodes.[26] As the water drop leaves the dual-mode TENG, the contacted surfaces are separated due to their own elastic resilience, then a negative EPD between the ITO electrode 1 and ITO electrode 2 (vii). This causes the electrons to flow from the ITO electrode 1 to ITO electrode 2, finally reaching equilibrium (viii). Once another charged water drop falls on the dual-mode TENG and makes the PTFE film contact with nylon film again, a negative EPD between ITO electrode 1 and ITO electrode 2 will be established, driving electrons flow from ITO electrode 2 to ITO electrode 1 (ix), until reaching another equilibrium (vi).[22] When water drops fall down and leave the dual-mode TENG periodically, an AC output will be generated from the contact TENG. As for wind contact TENG working mechanism, it is exactly the same with water contact TENG except for the driving force, i.e., one is the impact force from water drops, and the other is the impact force from wind.

It is essential to investigate the performance of dual-mode TENG for harvesting energy from natural raindrop and ambient wind. Here, we used water drops sprayed from a shower which is connected to a household faucet to simulate raindrops. The distance between the outlet of water drops and the dual-mode TENG surface is around 40 cm, and the water dripping rate was controlled at a rate of 13.6 mL s^{-1}. The incident angle between water dripping direction and TENG surface was set at 45°.[11] The typical output of J_{sc} and V_{oc} curves generated from output 1 and output 2 of dual-mode TENG impacted by water drops is displayed in **Figure 3**, where the values of J_{sc} and V_{oc} of water TENG and water contact TENG are 3.5 (Figure 3a) and 9.8 mA m^{-2} (Figure 3d) and 17.5 (Figure 3b) and 27.2 V (Figure 3e), respectively. Due to the fact that when countless water drops fall randomly on the PTFE film surface, not all the drops can reach or leave the PTFE film simultaneously, thus the curves of output voltage and current exhibit random fluctuating characteristics. Under the same experimental conditions, when we used a hydrophilic nylon film to replace the nanostructured PTFE film, the output J_{sc} of water TENG decreased sharply (Figure S2, Supporting Information), indicating that the superhydrophobic surface of PTFE film plays a critical role in prompting the removal of the water drops from TENG surface and can enhance the electric output of water TENG.

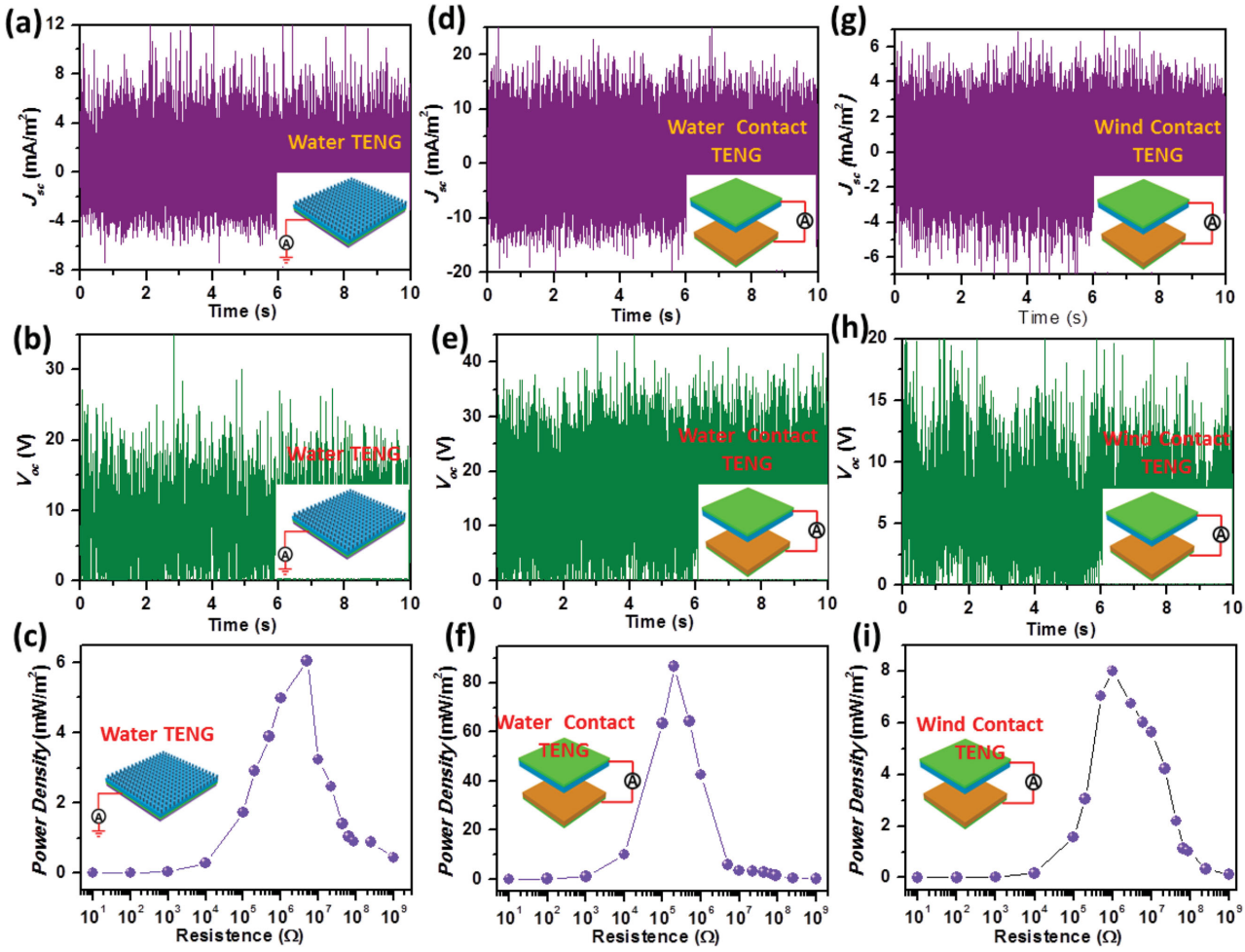

Figure 3. Generated a) J_{sc} and b) V_{oc} from output 1 of dual-mode TENG by water-PTFE electrification effects. Generated d) J_{sc} and e) V_{oc} from output 2 of dual-mode TENG under the impact of water drops from a shower connected with household faucet, where the dripping rate of water was set at 13.6 mL s^{-1}, and the distance between the dual-mode TENG and the shower was 40 cm. Generated g) J_{sc} and h) V_{oc} from output 2 of dual-mode TENG under the impact of wind blew from a wind faucet, where the wind speed is at 2.7 m s^{-1}. c,f,i) Dependence of average power density from output 1 and output 2 of dual-mode TENG on the resistance of the external load.

On the other hand, when the dual-mode TENG is blown by the natural wind, it will also cause the random contact and separation of the PTFE film with nylon film, which then generate continuous electrical output. To reveal the relationship between the output of wind contact TENG and wind speed numerically and perform this experiment in an easy way, we used a wind faucet in our lab to simulate the natural wind and fan the dual-mode TENG, where the wind speed can be controlled by a rotary knob and can be tested by an anemometer (Figure S3, Supporting Information). Under a speed of 2.7 m s^{-1} which is a very usual wind speed in our daily life, the basic output J_{sc} and V_{oc} values of wind contact TENG are 3.1 mA m^{-2} and 10.7 V, respectively, as shown in Figure 3g,h. With the increase of wind speed, the output of wind contact TENG will also increase, which will be investigated in detail in the following part of this paper.

To comprehensively characterize the demonstrated dual-mode TENG as a power source, resistors were utilized as external loads to measure the output voltage, current, and power of the dual-mode TENG. As displayed in Figure S4 (Supporting Information), the current amplitude drops with increasing load resistance owing to the ohmic loss, while the voltage follows a reverse trend. As a result, the average power density generated from output 1 and output 2 of dual-mode TENG remains small with the resistance below 0.01 MΩ and achieves the maximum values of 6 mW m^{-2} (Figure 3c), 86 mW m^{-2} (Figure 3f), and 8 mW m^{-2} (Figure 3i) at a resistance of 5, 0.2, and 1 MΩ, respectively.

The reported hybridized power panel can harvest solar, rain, and wind energy simultaneously or individually when either of them is available in the ambient environment, and this is a very beneficial compensation for solar energy harvesting itself. In sunny or cloudy days, the as-fabricated hybrid cell can harvest solar and wind energy simultaneously. **Figure 4**a shows that the output voltage of the Si solar cell under a light intensity of 100 mW cm^{-2} is around 0.6 V, while the output voltage of hybrid cell driven by sunlight and wind at speed of 2.7 m s^{-1} reaches nearly 11 V, where the solar cell and wind

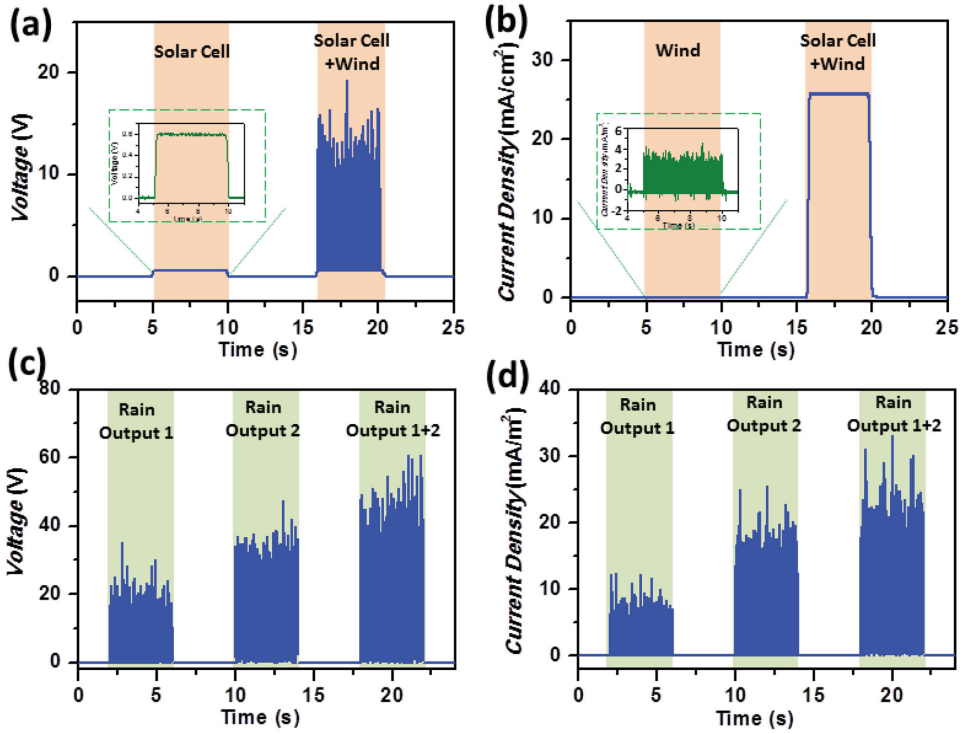

Figure 4. a) Output voltage of solar cell, and the hybridized power panel driven by wind at a speed of 2.7 m s^{-1} (solar cell and wind contact TENG in series) under a full sun condition. Inset shows the corresponding magnified curve of output voltage of solar cell. b) Output current density of wind contact TENG driven by wind at a speed of 2.7 m s^{-1} and the hybridized power panel (solar cell and wind contact TENG in parallel). Insets show the corresponding magnified curve of J_{sc} of wind contact TENG. c) Output voltage of water TENG, water contact TENG, and dual-mode TENG driven by water drops (output 1 and output 2 in series). d) Output current density of water TENG, water contact TENG, and dual-mode TENG impacted by water drops at a dripping rate of 13.6 mL s^{-1} (output 1 and output 2 in parallel).

contact TENG are connected in series after rectified by a full wave bridge circuit. The output current density of wind contact TENG is 3.1 mA m^{-2}, while the J_{sc} of hybrid cell where the solar cell and wind contact TENG are connected in parallel is 25.9 mA cm^{-2} (see Figure 4b), respectively. Compared with the J_{sc} from solar cell under a full sun condition, although the J_{sc} from wind contact TENG is relatively small, it is a good compensation for solar energy harvesting. However, always under a full sun is a realistic case because all of the solar cell panels have to be under normal sunlight at various weather conditions. In cloudy days, due to the great decrease of sunlight, the J_{sc} from wind contact TENG is approaching to the value of J_{sc} from solar cell and probably surpass it at night. And in addition, wind contact TENG can provide much higher output voltage than solar cell, and this is also useful in some real applications.

In rainy days, due to the dimness of sunlight, the functionality of solar cell is greatly depressed. But there are countless raindrops, and more importantly, the raindrops carry energies, i.e., the electrostatic energy gained from the contact with air/particles and the mechanical energy gained from gravitational force when falling in sky. In such circumstance, though the output of solar cell part is relatively small, our hybridized power panel can harvest both the raindrop electrostatic and mechanical energy using a dual-mode TENG, which is very meaningful for natural energy harvesting, especially in raining seasons.[32] In this experiment, we used water drops sprayed from a household shower to measure the output voltage and output current of the water TENG, water contact TENG, and dual-mode TENG driven by water drops at a dripping rate of 13.6 mL s^{-1}. From Figure 4c,d, we can see that both the output voltage and output current density of the water contact TENG are much higher than the water TENG itself, and this is due to a fact that the traditional contact electrification between two different dry materials is much stronger than water–solid triboelectric effect. By integrating the two outputs together, the hybridized power panel provides much higher output voltage and current density than either of the two working modes of the dual-mode TENG (Figure 4c,d), indicating a higher efficiency in harvesting raindrop energy.

For practical applications in driving LEDs or charging a capacitor, the electrical outputs of the water TENG and the water contact TENG are connected in parallel through a full-wave bridge. As the dual-mode TENG is driven by water drops at a dripping rate of 20 mL s^{-1}, ten commercial green LEDs are lighted up by the water TENG and 20 LEDs are lighted up by water contact TENG, respectively, as shown in **Figure 5**a. Combined with solar cell, 50 LEDs can be lighted up by the hybridized power panel driven by water drops under room light conditions. The dual-mode TENG is also demonstrated to charge a capacitor of 3.3 μF at a water dripping rate of 20 mL s^{-1}. As shown in Figure 5b, it takes 59 and 6.5 s to charge the capacitor to a voltage of 7 V by the water TENG and water contact TENG, respectively. The output power of contact TENG is much more efficient compared with the single water TENG under the same

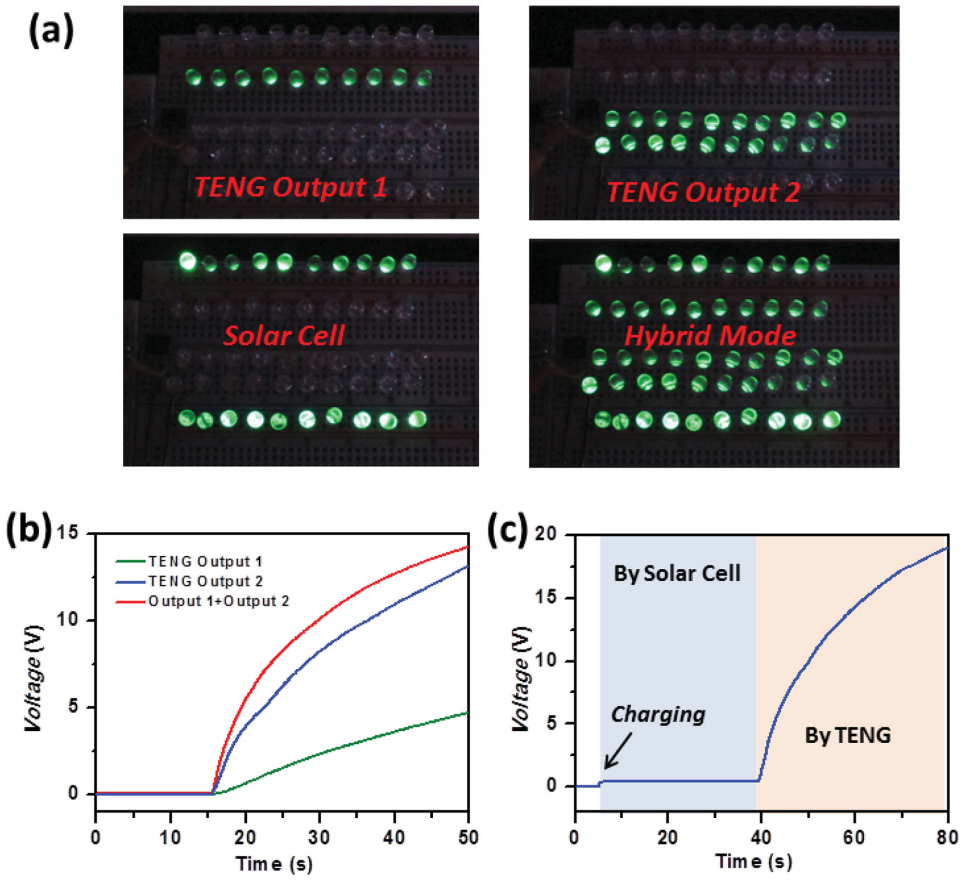

Figure 5. a) The photograph of 50 commercial LED bulbs driven by the hybridized power panel (10 LEDs lighted by water TENG, 20 LEDs by water contact TENG at a dripping rate of 20 mL s^{-1}, and 20 LEDs by solar cell). b) The measured voltage curves of a 3.3 μF capacitor charged by water TENG, water contact TENG, and dual-mode TENG, separately. c) The measured voltage curve of a 3.3 μF capacitor charged by the solar cell and dual-mode TENG impacted by water drops consequently.

experimental conditions. When using the dual-mode TENG, it takes 4.5 s to charge the capacitor to a voltage of 7 V. As for the comparison of the output voltage performance between solar cell and dual-mode TENG, the fabricated solar cell under a light illumination of 100 mW cm^{-2} was first used to charge the capacitor to a maximum of 0.6 V due to its upper voltage limit. Then the rectified dual-mode TENG was used to charge the same capacitor, it took 39 s to charge the capacitor to a voltage of 19 V and the corresponding curves are displayed in Figure 5c. The comparison results indicate that the hybridized power panel can compensate the lower voltage output of the solar cell itself.

Since the contact mode of TENG can also be driven by wind, the hybridized power panel can generate electricity from natural wind in the environment, which will further expand its applications. Here, we used the wind from a faucet with various speeds to drive the contact TENG, and the measured J_{sc} curve of the dual-mode TENG driven by wind at different speeds is shown in **Figure 6**a. Driven by the wind at a speed of 1.7 m s^{-1}, a common speed in our daily life, the output J_{sc} of dual-mode TENG reaches 1.3 mA m^{-2}. With the increase of the wind speeds, the output J_{sc} values were remarkably increased. The dependences of J_{sc} values of the dual-mode TENG on the wind speed are shown in Figure 6b, in which the J_{sc} values increase almost linearly with the wind speed till a saturated value of 9.2 mA m^{-2} is reached under a speed of 4.9 m s^{-1}. This linear increasing trend can also be calibrated as a self-powered sensor for natural wind speed monitoring.

3. Conclusion

In summary, we reported a hybridized power panel to generate electricity from solar, raindrops, and wind. By hybridizing a transparent dual-mode TENG with a common solar cell, the hybridized power panel can simultaneously/individually harvest solar, raindrop, and wind energy in various weather conditions around the clock. Without compromising the output performance of the original solar cell itself, the presented hybrid cell can, respectively, deliver an average output of 86 mW m^{-2} from the dripping water drops at a rate of 13.6 mL s^{-1}, and an average output of 8 mW m^{-2} at a wind speed of 2.7 m s^{-1}. This creative hybridization greatly expanded the device working time compared with the commonly used solar cell, playing an important and compensative role in the current field of solar energy harvesting. Given its exceptional properties of being cost-effective, easy fabrication, greatly expanded working time, and unique applicability resulting from distinctive device structure, the

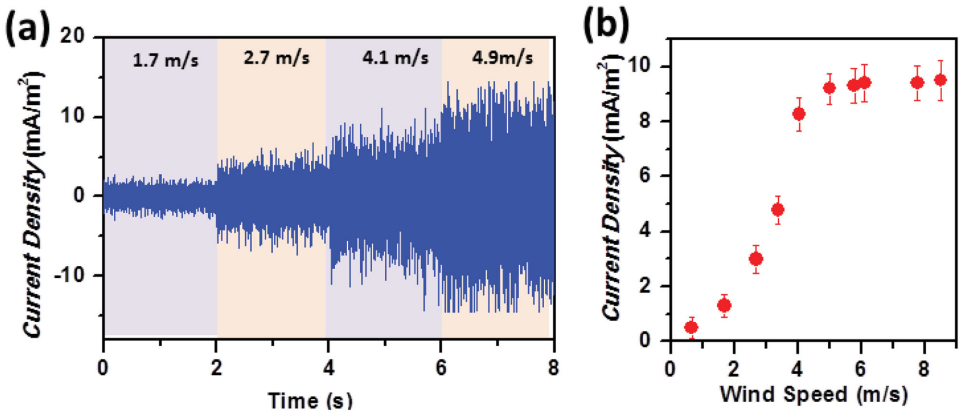

Figure 6. a) The J_{sc} curve at various wind speeds and b) the dependences of J_{sc} on wind speed of the dual-mode TENG when it is driven by wind.

hybridized power panel is a practical approach for higher efficiency ambient energy harvesting with lower production cost per watt. Additionally, the concepts and demonstrations in this work can be immediately and extensively adopted in the real industrial field of solar energy harvesting, and come into effect in improving our way of living.

4. Experimental Section

Fabrication of Si Solar Cell with Micropyramids: A 300 μm thick, single-crystal, p-type float-zone substrate was used as Si substrate, then the Si wafer was etched by KOH solution to form textured surface. After cleaning, the wafer was followed by $POCl_3$ diffusion to form n^+ emitters, where a diffusion temperature of 1133 K was used to obtain a 65 Ω sq^{-1} emitter. Via a plasma-enhanced chemical vapor deposition reactor, the wafer was then coated with 80 nm SiN film, which serves as a passivation and antireflection coating layer. After that, an Al paste was screen-printed on the backside of the Si substrate and dried at 473 K. Ag grids were then screen-printed on top of the Si substrate, followed by cofiring of both the Ag and Al contacts. At last, an ITO top electrode was coated by PVD 75 RF sputter.

Fabrication of the Hydrophobic PTFE Film: First, microstructures were fabricated by blasting an Al foil with sand particles using compressed air. The sand-blasted Al foil was further anodized in a 0.3 M oxalic acid solution to obtain an AAO template with nanometer-sized holes. Then after using a self-assembled monolayer of an HDFS to lower the surface energy of the AAO template, PTFE solution was poured into the AAO template, and a conventional vacuum process was applied to remove the air remaining in the nanoholes. After curing at the ambient temperature for a whole day, the solvent was evaporated and left a PTFE thin film with hierarchical nanostructures. Finally, the PTFE thin film was peeled off from the AAO template by using a transparent double-sided tape.

Fabrication of Hybrid Cell: A thin layer of ITO was deposited on the fabricated superhydrophobic PTFE film as electrode by the e-beam evaporation to form a water TENG. Meanwhile, a piece of commercial PTFE film with thickness of 25 μm and a piece of nylon film was deposited with ITO by e-beam evaporation as electrodes, respectively. Then the PTFE and nylon film with ITO electrodes outside are integrated by a PET spacer to form a contact TENG. A thin layer of PDMS mixture with elastomer and cross-linker (Sylgard 184, Dow Corning) mixed in a 10:1 mass ratio was used to agglutinate the water TENG and contact TENG together to form a dual-mode TENG. Then the fabricated dual-mode TENG was put on the surface of Si-based solar cell. Finally, some PDMS mixture and epoxy was used to seal all the electrodes of the device to prevent the device from water and natural corrosions.

Measurement of Hybrid Cell: The solar cell efficiency was characterized under the light illumination intensity of 100 mW cm^{-2}. The *J–V* curves of Si-based solar cell integrated with conventional glass and dual-mode TENG were measured by using a Keithley 4200 semiconductor characterization system, respectively. The spectra transmittance of 3 mm thick glass and dual-mode TENG were measured by a UV–vis spectrophotometer (V-630). The current meter (SR570 low noise current amplifier, Stanford Research System) and voltage meter (Keithley 6514 System Electrometer) were used to measure the electric outputs of the water TENG, water contact TENG, and wind contact TENG.

Supporting Information

Supporting Information is available from the Wiley Online Library or from the author.

Acknowledgements

L.Z., G.C., and J.C. contributed equally to this work. This work was supported by U.S. Department of Energy, Office of Basic Energy Sciences (Award No. DE-FG02-07ER46394), the Hightower Chair foundation, Innovation Program of Shanghai Municipal Education Commission (13YZ104), National Natural Science Foundation of China (Nos. 11204172, 11374204), and the "Thousands Talents" program for pioneer researcher and his innovation team, China, Beijing City Committee of Science and Technology (Z131100006013004, Z131100006013005).

Received: June 10, 2015
Published online:

[1] H. Meyar-Naimi, S. Vaez-Zadeh, *Energy Policy* **2012**, *43*, 351.
[2] N. S. Lewis, *Science* **2007**, *315*, 798.
[3] B. Tian, X. Zheng, T. J. Kempa, Y. Fang, N. Yu, G. Yu, J. Huang, C. M. Lieber, *Nature* **2007**, *6*, 885.
[4] P. Devine-Wright, *Wind Energy* **2005**, *8*, 125.
[5] Z. L. Wang, J. Song, *Science* **2006**, *312*, 242.
[6] Y. Qin, X. Wang, Z. L. Wang, *Nature* **2008**, *451*, 809.
[7] G. Zhu, J. Chen, T. J. Zhang, Q. S. Jing, Z. L. Wang, *Nat. Commun.* **2014**, *5*, 3426.
[8] Y. Yang, H. Zhang, Z. H. Lin, Y. Liu, J. Chen, Z. Lin, Y. Zhou, C. P. Wong, Z. L. Wang, *Energy Environ. Sci.* **2013**, *6*, 2429.

[9] J. Chen, J. Yang, Z. Li, X. Fan, Y. Zi, Q. Jing, H. Guo, Z. Wen, K. C. Pradel, S. Niu, Z. L. Wang, *ACS Nano* **2015**, 9, 3324.
[10] Y. Liu, A. Das, S. Xu, Z. Y. Lin, C. Xu, Z. L. Wang, A. Rohatgi, C. P. Wong, *Adv. Energy Mater.* **2012**, *2*, 47.
[11] L. Zheng, Z.-H. Lin, G. Cheng, W. Z. Wu, X. N. Wen, S. Lee, Z. L. Wang, *Nano Energy* **2014**, *9*, 291.
[12] F. R. Fan, Z. Q. Tian, Z. L. Wang, *Nano Energy* **2012**, *1*, 328.
[13] K. Y. Lee, J. Chun, J. Lee, K. N. Kim, N. R. Kang, J. Y. Kim, M. H. Kim, K.-S. Shin, M. K. Gupta, J. M. Baik, S.-W. Kim, *Adv. Mater.* **2014**, *26*, 5037.
[14] Y. Zi, L. Lin, J. Wang, S. Wang, J. Chen, X. Fan, P. K. Yang, F. Yi, Z. L. Wang, *Adv. Mater.* **2015**, 27, 2340.
[15] G. Cheng, Z.-H. Lin, L. Lin, Z. Du, Z. L. Wang, *ACS Nano* **2013**, *7*, 7383.
[16] J. Chen, G. Zhu, J. Yang, Q. Jing, P. Bai, W. Yang, X. Qi, Y. Su, Z. L. Wang, *ACS Nano* **2015**, *9*, 105.
[17] G. Cheng, L. Zheng, Z.-H. Lin, J. Yang, Z. L. Du, Z. L. Wang, *Adv. Energy Mater.* **2015**, *5*, 1401452.
[18] J. Yang, J. Chen, Y. Yang, H. Zhang, W. Yang, P. Bai, Y. Su, Z. L. Wang, *Adv. Energy Mater.* **2014**, *4*, 1301322.
[19] G. Cheng, Z.-H. Lin, L. Lin, Z. L. Du, Z. L. Wang, *ACS Nano* **2013**, *7*, 7383.
[20] Z.-H. Lin, G. Cheng, L. Lin, S. Lee, Z. L. Wang, *Angew. Chem.* **2013**, *125*, 12777.
[21] G. Zhu, B. Peng, J. Chen, Q. Jing, Z. L. Wang, *Nano Energy* **2015**, 14, 126.
[22] Z.-H. Lin, G. Cheng, S. Lee, Z. L. Wang, *Adv. Mater.* **2014**, *26*, 4690.
[23] G. Zhu, Y. Su, P. Bai, J. Chen, Q. Jing, W. Yang, Z. L. Wang, *ACS Nano* **2014**, *8*, 6031.
[24] S. Lee, J. H. Kang, S. J. Lee, W. H. Wang, *Lab Chip* **2009**, *9*, 2234.
[25] C. R. Crick, I. P. Parkin, *Chem. Commun.* **2011**, *47*, 12059.
[26] J. Chen, G. Zhu, W. Yang, Q. Jing, P. Bai, Y. Yang, T. C. Hou, Z. L. Wang, *Adv. Mater.* **2013**, *25*, 6094.
[27] D. Choi, H. Lee, D. J. Im, I. S. Kang, G. Lim, D. S. Kim, K. H. Kang, *Sci. Rep.* **2013**, *3*, 2037.
[28] B. Ravelo, F. Duval, S. Kane, B. Nsom, *J. Electrost.* **2011**, *69*, 473.
[29] G. Zhu, P. Bai, J. Chen, Z. L. Wang, *Nano Energy* **2013**, *2*, 688.
[30] J. Yang, J. Chen, Y. Liu, W. Yang, Y. Su, Z. L. Wang, *ACS Nano* **2014**, *8*, 2649.
[31] G. Cheng, Z.-H. Lin, Z. Du, Z. L. Wang, *Adv. Funct. Mater.* **2014**, *24*, 2892.
[32] Q. Liang, X. Yan, Y. Gu, K. Zhang, M. Liang, S. Lu, X. Zheng, Y. Zhang, *Sci. Rep.* **2015**, *5*, 9080.